

Proteasomal Degradation of Proteins Is Important for the Proper Transcriptional Response to Sulfur Deficiency Conditions in Plants

Anna Wawrzyńska* and Agnieszka Sirko

Institute of Biochemistry and Biophysics Polish Academy of Sciences, Pawinskiego 5A St, 02-106 Warsaw, Poland

*Corresponding author: E-mail, blaszczyk@ibb.waw.pl; Fax, +48 22 5922190.
(Received 6 February 2020; Accepted 29 May 2020)

Plants are continuously exposed to different abiotic and biotic stresses; therefore, to protect themselves, they depend on the fast reprogramming of large gene repertoires to prioritize the expression of a given stress-induced gene set over normal cellular household genes. The activity of the proteasome, a large proteolytic complex that degrades proteins, is vital to coordinate the expression of such genes. Proteins are labeled for degradation by the action of E3 ligases that site-specifically alter their substrates by adding chains of ubiquitin. Recent publications have revealed an extensive role of ubiquitination in the utilization of nutrients. This study presents the transcriptomic profiles of sulfur-deficient rosettes and roots of *Arabidopsis thaliana rpt2a* mutant with proteasomal malfunction. We found that genes connected with sulfur metabolism are regulated to the lesser extent in *rpt2a* mutant while genes encoding transfer RNAs and small nucleolar RNAs are highly upregulated. Several genes encoding E3 ligases are specifically regulated by sulfur deficiency. Furthermore, we show that a key transcription factor of sulfur deficiency response, Sulfur LIMitation1, undergoes proteasomal degradation and is able to interact with F-box protein, EBF1.

Keywords: 26S proteasome • *Arabidopsis thaliana* • SLIM1 • Sulfur starvation • Transcriptome analysis • Ubiquitination.

Accession number: The microarray data described in the article have been deposited in Gene Expression Omnibus (<https://www.ncbi.nlm.nih.gov/geo>, (June 16, 2020, date last accessed)) and are accessible through GEO Series accession number GSE 137728.

Introduction

To adapt to and survive unfavorable and unexpected changes in their environment, plants maintain a high level of growth plasticity throughout their lifetime. Numerous biotic and abiotic stresses are continually challenging them because of their sessile nature. The stresses trigger responses that reprogram and adjust

metabolism, growth and development. The plants use a combination of checks on transcriptional, posttranscriptional, translational and posttranslational gene expression levels to respond to diverse environmental conditions (Des Marais and Juenger 2010, Walley and Dehesh 2010, Vaahtera and Brosche 2011). Accumulating data show the significance of targeted protein degradation mechanisms in the response to abiotic and biotic stresses in plant metabolism. Signaling mechanisms during stresses involve explicit timing control, which explains why crops often depend on selective protein degradation, particularly ubiquitination that leads to proteasomal degradation. The primary benefits are the speed and commitment of signaling based on ubiquitination. Ubiquitin-tagged substrates have their half-lives expeditiously reduced with fast steady-state level changes caused by particular stimuli. Improper reactivation is also prevented by the irreversible removal of modified proteins.

Ubiquitin is a very stable, small 76-amino-acid peptide that is highly conserved throughout eukaryotes. Ubiquitin attachment to protein may affect its activity, abundance, trafficking or location. This versatility of function is based on the different ways in which ubiquitin molecules can be attached to a particular protein (Komander and Rape 2012). Ubiquitin includes seven residues of lysine that can each be used to create ubiquitin–ubiquitin linkages producing structurally diverse polyubiquitin chains. Lysine 48-linked chains of four or more ubiquitins show a high affinity for ubiquitin receptors within the 19S regulatory cap of the proteasome (Thrower et al. 2000). The regulatory particle forms a so-called base and lid structure. The base contains six related AAA-ATPases (RPT1–6) and three non-ATPase units (RPN1, 2 and 10), while the lid, which interacts with the base through RPN10, contains the remaining non-ATPases (RPN3, 5–9, 11 and 12). After unfolding, the substrate is threaded into the 20S subunit of the proteasome, a barrel-shaped multi-catalytic proteinase, while the polyubiquitin chain is released for recycling (Pickart and Cohen 2004). The whole 26S proteasome complex is present in the cytoplasm and in the nucleus (Wojcik and DeMartino 2003). The 26S proteasomes are indispensable for cell survival, and only weak loss-of-function mutants (*rpt2a-2*, *rpt2a-3*, *rpn10-1* or *rpn12a-1*) can be generated (Kurepa et al. 2009).

There are three main steps leading to the ubiquitination of target proteins, each needing a distinct enzyme that acts hierarchically with other enzymes: ubiquitin-activating (E1s), ubiquitin-conjugating (E2s) and ubiquitin ligase (E3s) enzymes (Sharma et al. 2016). The cascade begins with the activation of ubiquitin in an ATP-dependent reaction to form an E1-ubiquitin thioester-linked intermediate. The E1-ubiquitin interacts with the E2 to enable the transfer of the activated ubiquitin, thus forming a thioester-linked E2-ubiquitin intermediate. The enzyme E3 promotes the immediate transfer of ubiquitin to the target protein as it interacts with both the E2-ubiquitin and the target protein. This final step connects the C-terminal glycine carboxyl group of ubiquitin to lysine through an isopeptide bond. After the initial ubiquitin molecule has been attached, the process can be repeated to assemble a poly-ubiquitin chain (Komander and Rape 2012).

The substantial dependence of plants on protein ubiquitination to control organismal processes becomes apparent after sequencing their genomes. More than 6% of *Arabidopsis thaliana* protein-coding genes are devoted to ubiquitin–proteasome system (UPS) (Vierstra 2009). While *Arabidopsis* encodes for only 2 E1s and 37 E2s, it can theoretically express over 1,300 different E3s (Vierstra 2009). This enormous amount of predicted E3s in *Arabidopsis* is one of the plant kingdom's largest collections of enzymes, illustrating the significance of ubiquitination to plant biology. Plant E3 ubiquitin ligases are highly diverse as they constitute the main variables that determine substrate specificity (Mazzucotelli et al. 2006). There are three main E3 types in plants: based on their action mechanisms and subunit organization: HECT (Homology to E6-Associated Carboxy-Terminus), RING (Really Interesting New Gene)/U-box and multi-subunit CRL (Cullin-RING ligases) E3s (Hua and Vierstra 2011). Plant CRLs utilize substrate-recruiting proteins belonging to either the F-box (700 members), the BTB (Broad Tramtrack Bric-a-Brac Complex 80 members) or DWD (DDB1 binding WD40; 85 members) families (Stone 2014). The diverse combination of E1s, E2s and E3s offers specificity to thousands of proteins each uniquely targeted so that countless cellular processes can be tightly controlled.

E3 ubiquitin ligases are actively involved in hormone perception and signaling pathways, degradation of hormone-specific transcription factors and hormone biosynthesis regulation (Santner and Estelle 2010). Hormones function to integrate diverse environmental clues with endogenous growth programs. Most of them are involved in multiple processes and affect each other through multileveled crosstalk strategies (Santner and Estelle 2010). There is ample evidence of one hormone regulating the expression of genes involved in the metabolism of another hormone, particularly in the areas of growth regulation and stress response (Stone 2014). The UPS elements engaged in hormonal signaling regulation can also be part of the response to nutrient deficiency conditions due to a high interference of the environmental cues with hormonal signaling. The significance of the ubiquitination pathway in abiotic stress tolerance has been indicated by the finding that the expression of the ubiquitin gene in plants subjected to elevated temperature stress is upregulated (Genschik et al. 1992, Sun and

Callis 1997). Mutations of the 26S proteasome regulatory subunit, affecting its function, may decrease complex accumulation and reduce the rate of ubiquitin-dependent proteolysis, resulting in hypersensitivity to salt and osmotic stresses of the corresponding *Arabidopsis* mutant lines (Smalle et al. 2003, Smalle and Vierstra 2004). UPS has been shown to control the response of plants to elevated temperatures, UV irradiation, salt and drought (Lyzena and Stone 2012). Recent studies have disclosed that in addition to its extensive role in stress signaling, ubiquitination followed by selective degradation is essential for the utilization of nutrients. The data highlighting the role of UPS in the ability of plants to uptake and process nutrients are still very limited and concern few examples of carbon, nitrogen, phosphorus, zinc and iron metabolism (Peng et al. 2007, Sato et al. 2009, Long et al. 2010, Lingam et al. 2011, Sakamoto et al. 2011, Sato et al. 2011, Liu et al. 2012, Pratelli et al. 2012, Lin et al. 2013, Shin et al. 2013, Pan et al. 2019).

Growth of healthy, high-yielding crop plants requires a stable input of yet another nutrient: sulfur (S). The growing awareness for the significance of plant S nutrition has attracted the attention of many researchers; therefore, our knowledge about S metabolic pathways and regulatory aspects of S assimilation has expanded significantly during the last decades. The biochemistry of S assimilation is well characterized; however, there are still many unresolved questions regarding the regulation of S metabolism in response to both the availability of S in the environment and the increased demand of plants for S metabolites under certain environmental conditions (e.g. UV irradiation or heavy metals contamination inducing oxidative stress and the need for higher synthesis rate of glutathione). With the prevalent occurrence of S deficiency in soils, it is essential to comprehend the molecular processes of plant responses to changing S nutrition conditions. Therefore, particular attention has been given to plant responses to S starvation, including transcriptomics and metabolomics approaches (Wawrzyńska et al. 2005, Watanabe and Hoefgen 2019). A general outcome of these works is that multilevel regulation is required to adjust the entire S flux to fulfill the new demands. Besides gene expression also translation efficiency, the activity of enzymes needed for sulfate assimilation and synthesis of S metabolites are regulated (Takahashi et al. 2011). The molecular bases of these regulations remain largely unknown.

Regulation of gene expression at the transcription stage is a major control point in many biological processes (BPs); however, the only trans-acting factor specifically regulating the transcription of the genes during S deficiency identified so far is SLIM1 (Sulfur LIMitation1) from *Arabidopsis* (Maruyama-Nakashita et al. 2006). SLIM1 belongs to a small plant-specific multigenic family of which several members were cloned and described in distinct species (Wawrzyńska and Sirko 2014). Six genes are annotated in the *Arabidopsis* genome to encode the EIL [Ethylene INsensitive3 (Eln3)-Like] family proteins with the best-characterized member being EIN3 (Guo and Ecker 2004). The transcription factor EIN3, together with its functional homologs EIL1 and EIL2, controls the expression of ethylene-responsive genes (Chao et al. 1997, Solano et al. 1998). Many reports have highlighted the role of UPS in ethylene signaling.

Three groups independently discovered that EIN3 is ubiquitinated by interaction with two E3 proteins, EBF1 and EBF2 (Ein3 Binding F-box), and is therefore aimed at the 26S proteasome (Potuschak et al. 2003, Gagne et al. 2004, Guo and Ecker 2004). EBF1 acts constitutively at a low concentration of ethylene, thus repressing the ethylene response pathway. EBF2 works mainly in silencing the signal, after its activation by withdrawing EIN3, so the plants can resume normal growth more quickly (Binder et al. 2007). Other signals, such as glucose, light, phosphorylation and jasmonate, quantitatively regulate the amount of EIN3 (Wawrzyńska and Sirko 2014), although the precise mechanisms of degradation are not yet identified. SLIM1 transcription is not influenced by S deficiency, so it is sensible to speculate that SLIM1 may involve posttranscriptional/post-translational processes to regulate its performance, comparable to its close EIN3 homolog. However, not much is known about posttranslational modifications in SLIM1 and the influence of ubiquitination on its stability. Unlike EIN3, whose protein level in the nucleus is affected by the stabilizing ethylene signal that blocks the action of EBF1 (Guo and Ecker 2003, Potuschak et al. 2003), S levels have not been known to alter the nuclear localization or abundance of SLIM1 protein tagged with Green Fluorescent Protein (GFP) in Arabidopsis seedlings (Maruyama-Nakashita et al. 2006).

As there is an increasing understanding of UPS participation in nutrient deficiency response, its input to the S metabolism can be anticipated. Nevertheless, no reports connecting UPS with metabolism reprogramming due to S deficiency stress are available. Therefore, we decided to investigate the consequences of proteasome malfunction in Arabidopsis in S-deficient conditions. We discovered that the proper response to S deficiency is impaired due to the mutation of one of the proteasome regulatory proteins, RPT2A. This mutation affects the assembly and accumulation of the 26S proteasome resulting in reduced rates of UPS-dependent proteolysis (Kurepa et al. 2008). Studies in yeast revealed that RPT2 is necessary for the channel opening of the core proteasomal complex, and thus for proteasome activity (Kohler et al. 2001). In Arabidopsis, RPT2a is essential for maintaining root and shoot apical meristems' cellular organization and plays an important role in response to zinc deficiency and pathogens (Ueda et al. 2004, Sakamoto et al. 2011, Üstün et al. 2016). We further examined the stability of SLIM1 protein and its ability to interact with E3 ubiquitin ligases. In this capacity, we propose that ubiquitination and subsequent selective protein degradation undoubtedly have a role in adjusting plant metabolism to lower sulfur supply.

Results

Transcriptome response of *rpt2a* mutant to S deficiency

To examine the role of the proteasome during S deficiency, we compared transcriptional changes between 5-week-old Arabidopsis Columbia-0 (wild type, WT) and *rpt2a* mutant plants subjected to 5-day S starvation. The stressed plants did not show any S deficiency phenotype. Microarray chip

hybridization was performed with the RNA isolated from rosettes and roots separately. The principal component analysis showed extensive clustering of the transcriptome data among the three samples from WT nS, WT dS, *rpt2a* nS and *rpt2a* dS (Supplementary Fig. S1). These results indicated that the transcriptome profile data were of sufficient quality to permit robust statistical analysis and interpretation.

First, we analyzed the S deficiency-responsive genes in the WT. The microarray data obtained from control WT were compared with that of S-starved WT. Most importantly, the S starvation stress was sensed by the plants as the S deficiency marker genes, *SDI1* (At5g48850) and *LSU1* (At3g49580) (Sirko et al. 2014, Aarabi et al. 2016), showed clear induction in rosettes and root tissue (Supplementary Table S3). Differentially expressed genes (DEGs) were defined as those with at least ± 1.5 -fold difference in expression and P -values ≤ 0.05 in comparison to WT grown in nS (Supplementary Table S3). We observed that the transcript levels of 336 and 484 genes changed significantly in S-starved rosettes and roots, respectively. Of these, in rosettes, 171 genes were identified as upregulated and 165 genes were qualified as downregulated by S starvation (Fig. 1B). Moreover, in roots, 303 genes were identified as upregulated and 181 genes were qualified as downregulated by S starvation (Fig. 1B). Remarkably, the number of

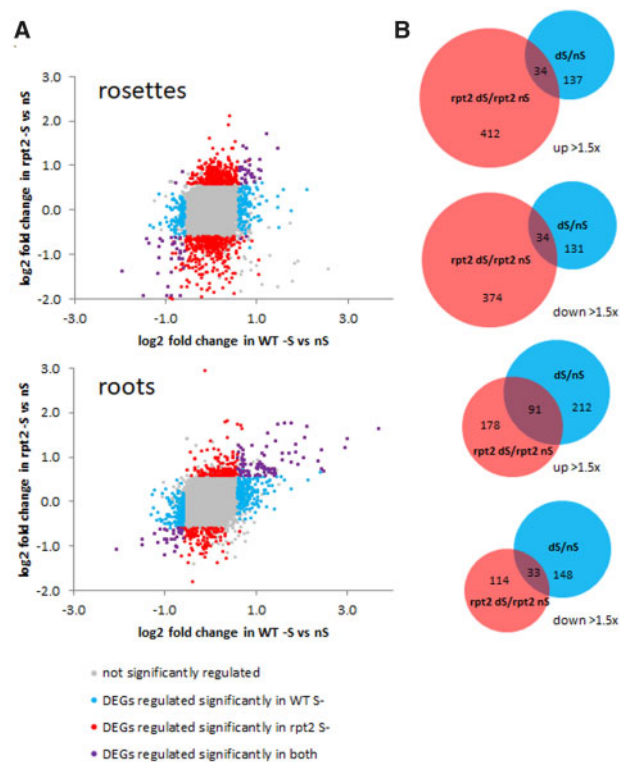


Fig. 1 Comparative analysis of transcriptome profiles of 5-week-old WT and *rpt2a* Arabidopsis rosettes and roots under normal (nS) and 5-day S deficiency (dS). (A) Scatter plots and (B) Venn diagrams showing the overlap of upregulated or downregulated genes in response to 5 d of S deficiency in WT (blue), *rpt2a* (red) and both (purple). The number of the DEGs (1.5-fold difference at $P \leq 0.05$) is shown for each circle.

overlapping DEGs between the two plant tissues was very small, prompting us to analyze the two data sets separately.

To elucidate the importance of proteasome during S starvation, we next compared the transcriptional changes in *rpt2a* mutant challenged with S deficiency. In rosettes, of the 854 DEGs, 446 were upregulated and 408 were downregulated, while in roots, out of the 416 DEGs, 269 were upregulated and 147 were downregulated (Fig. 1B and Supplementary Table S3). Notably, rosettes of *rpt2a* mutant showed much more variation in gene expression than that of WT and shared only 68 common DEGs (Fig. 1A, B). For roots, the number of DEGs was of similar size for each genotype; however, only about one-quarter of the genes contributed to the common part (Fig. 1A, B). The higher number of DEGs observed in *rpt2a* rosettes might reflect the fact that *rpt2a* plants show different expressions of 891 genes in comparison to WT, even in non-S-starved conditions (Supplementary Fig. S2), underlining the necessity of properly functioning 26S proteasomes for plant metabolism.

We performed a gene ontology (GO) analysis of DEGs using the functional annotation chart of the web-based tool agriGo v2.0. The BP GO classification of the DEGs for the WT and *rpt2a* plants identified 13 common GO terms ($P \leq 0.01$, Fig. 2, red bars) for rosettes and 9 for roots (Supplementary Fig. S3). Among the categories associated with DEGs in rosettes, 'primary' and 'secondary metabolic processes' and 'response to stimulus' were

significantly overrepresented. Interestingly, 'gene expression', 'protein metabolic process' and 'translation' were especially enriched in *rpt2a* mutant, whereas 'regulation of gene expression', 'response to ethylene' and 'sulfur compound metabolic process' were better represented in the WT plants (Fig. 3). In roots, 'regulation of gene expression' and 'sulfur compound metabolic process' were again categories with augmented DEGs frequencies, mostly for WT plants (Supplementary Figs. S3, S4).

Sulfur metabolism-connected genes show milder response in *rpt2a* mutant

It is now widely known that a single stressor, such as nutrient deficiency (e.g. S starvation), will affect not only S metabolism per se but also other interconnected and downstream processes. However, the GO category 'sulfur compound metabolic process' appeared to be enriched but mostly in the WT rosettes and roots. There are 474 genes assigned to the 'sulfur compound metabolic process' GO category. Surprisingly, we noticed that genes from this GO category were generally less regulated in *rpt2a* mutant. Despite the observed overreaction to S starvation of the *rpt2a* rosette transcriptomes in comparison to the WT plants, there were fewer genes with expression changed to the lesser extent that were actually connected with S metabolism (Fig. 4A and Supplementary Table S4). This phenomenon was even more visible for the root tissue (Fig. 4B and

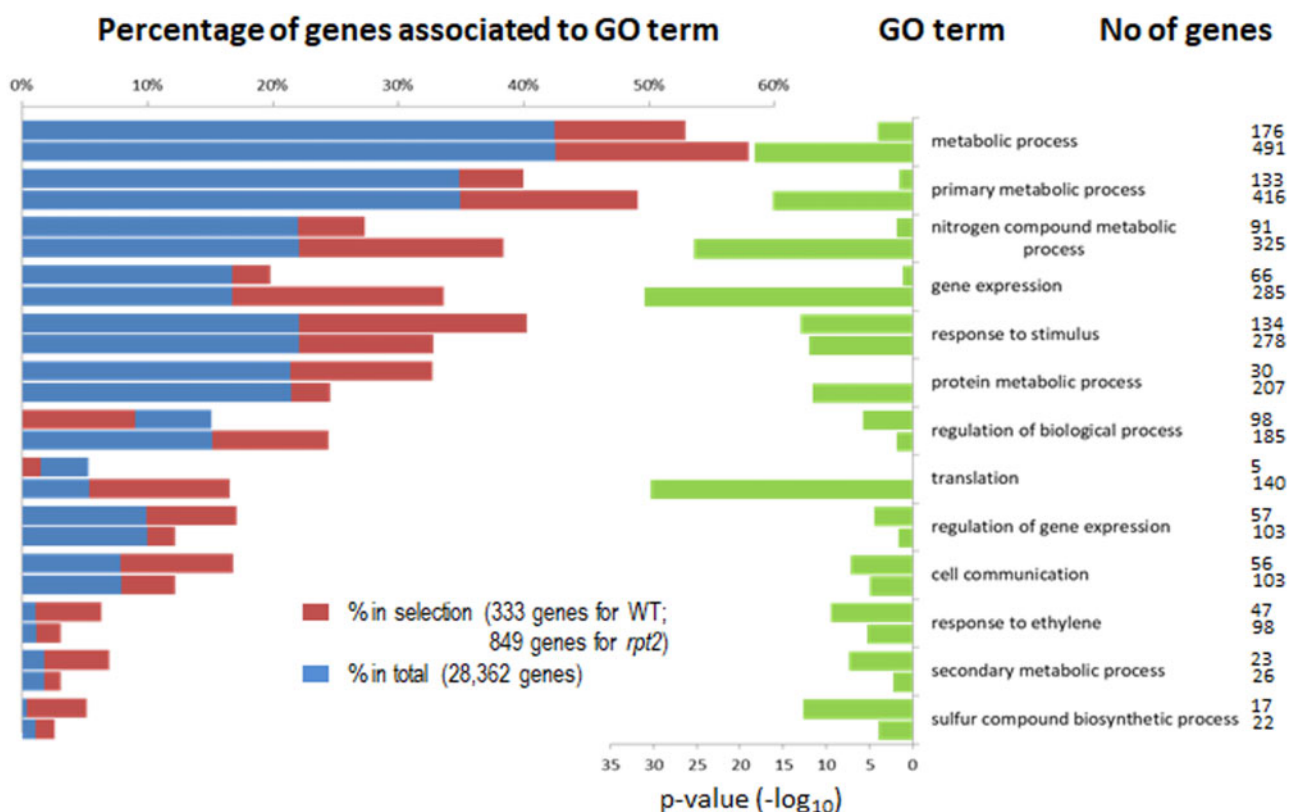


Fig. 2 GO enrichment analysis of the rosettes 333- and 849-gene set for the WT and *rpt2a* plants, respectively, regulated significantly by S deficiency. The percentages of genes that are associated with a GO term are shown in the left bars for the sets of 331 and 849 DEGs and for the total set of 28,362 genes. Enrichment scores (P -values) are represented by the bar graph in the right. The number of genes associated with each GO term is shown in the right column. Only GO terms in the category of BP are shown. The upper bar for each category represents the WT gene set while the lower bar represents the *rpt2a* gene set.

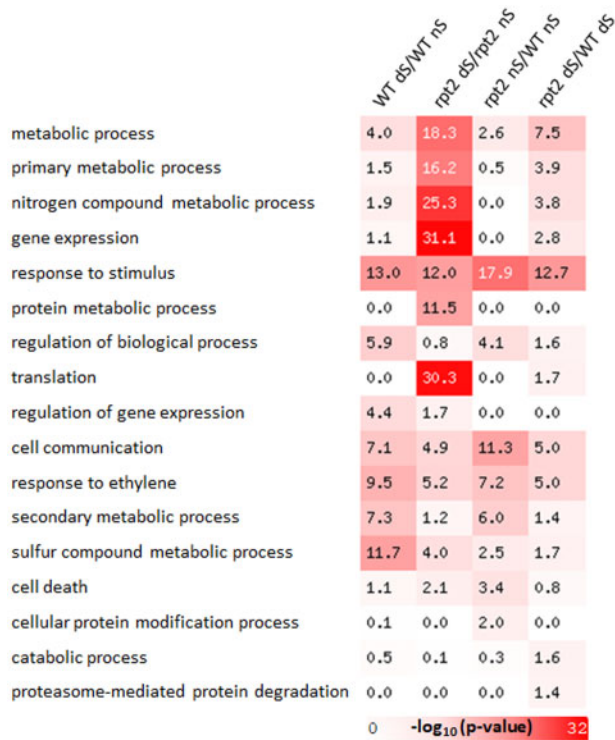


Fig. 3 Heat map showing *P*-value significance of enriched GO categories for DEGs (both upregulated and downregulated) for S deficiency in the WT (WT dS/WT nS) and *rpt2a* (rpt2 dS/rpt2 nS) plants and proteasomal downregulation in nS (rpt2 nS/WT nS) and dS (rpt2 dS/WT dS) in rosettes. BP enrichment analysis indicates that GO terms related to ‘gene expression’ and ‘translation’ were overrepresented in *rpt2a* mutant during S deficiency. The color scale of the *P*-value is presented below the heat map.

Supplementary Table S4), where only 49 genes were significantly regulated in *rpt2a* mutant as compared to the 91 regulated by S starvation in the WT plants. To confirm whether this observation resulted from proteasomal malfunction and not only the specific mutation in RPT2A, the expression of the five mostly misregulated genes was assayed with quantitative real-time PCR (qRT-PCR) in the seedlings of other proteasomal mutants, namely *rpn10* and *rpn12a*, S-starved for 4, 6 and 9 d (**Supplementary Fig. S5**). The transcription level of *SDI1*, *LSU1*, *ChaC*, *bGlu28* and *Sultr2;1* was indeed lower in all three proteasomal mutants than the WT but only after 4 and 6 d of S deficiency. On day 9, the expression levels of all the five genes were not significantly different from the WT (**Supplementary Fig. S5**). Since all three proteasomal mutations impaired the early transcriptional response to S deficiency, we tested whether the mutants are sensitive to extended sulfur starvation. The root length, fresh weight and anthocyanin content were affected in a similar way in all three mutants and the WT seedlings after 14 d of S starvation (**Supplementary Fig. S6**).

Transcription and translation are enhanced by proteasome malfunction in S-deficient rosettes

Two GO terms, ‘gene expression’ and ‘translation’, were significantly overrepresented in the group of DEGs regulated in

rosettes, but only in the *rpt2a* mutant background (**Figs. 2, 3** and **Supplementary Table S4**). The main contributors to those categories were small nucleolar RNA (snoRNA) and pre-transfer RNA (tRNA) genes, both being significantly upregulated. The change in the expression level of ‘gene expression’ and ‘translation’ GO categories genes in the rosettes of the WT plants and *rpt2a* mutant was illustrated with volcano plots (**Fig. 5A, B**). There are 426 pre-tRNA genes according to the TAIR10 Arabidopsis genome release. After trimming them to 155 genes encoding transcripts that could be differentiated by means of microarray hybridization, 77 transcripts showed upregulation and only 7 were downregulated. Among the upregulated transcripts, tRNAs with anticodons for asparagine, glutamine, glycine, histidine and tryptophan showed specific enrichment (**Supplementary Fig. S7**). To estimate the translation efficiency, the total level of proteins was assayed in rosettes and roots but also in 7- and 14-day S-starved seedlings of the WT plants and *rpt2a* mutant. No significant differences were noticed apart from clear inhibition of translation in long-term S-starved seedlings of both genotypes (**Supplementary Fig. S8**).

Transcription factors’ expression driven by S deficiency is repressed in *rpt2a* mutant roots

Analysis of GO term enrichment showed that in the WT roots, in addition to the ‘sulfur compound metabolic process’, the ‘regulation of gene expression’ is specifically enhanced (**Supplementary Figs. S3, S4**). We do not observe such situations in *rpt2a* mutant roots, which is clearly depicted by volcano plots (**Fig. 6A**). The category ‘regulation of gene expression’ includes 2,864 genes, encoding mostly transcription factors of different families. Results show that 78 transcription factors within more than five families were differentially expressed due to S deficiency (**Fig. 6B** and **Supplementary Table S4**). Of these, the ethylene response factor (ERF), basic helix–loop–helix (bHLH), MYB, NAC and WRKY families of genes made up of the four most abundant DEGs. Whereas 14 members of the bHLH family, as well as 8 members of the MYB family, exhibited increased patterns of expression under S starvation stress, 10 members of the ERF family and 5 members of the WRKY were downregulated. Only 40 genes encoding transcription factors were regulated in *rpt2a* mutant under the same conditions (**Fig. 6B**). Interestingly, among those, there are no members of the MYB gene family, while in the WT plants there are 11 genes, mostly belonging to the R2R3 type.

Expression of several UPS genes is affected by S deficiency

We were interested in whether S deficiency affects the expression level of any of the components of the ubiquitination cycle; therefore, we checked the regulation of all genes encoding E1, E2 and E3 enzymes. Interestingly, different genes were regulated in response to S starvation in rosettes and roots of the WT plants and *rpt2a* mutant (**Supplementary Fig. S9**). While in rosettes, there were only nine genes regulated in the WT plants compared to 30 in *rpt2a* mutant, the opposite reaction was observed for root tissue, with 21 genes for the WT plants and only 8 genes for the *rpt2a* mutant showing changed expression

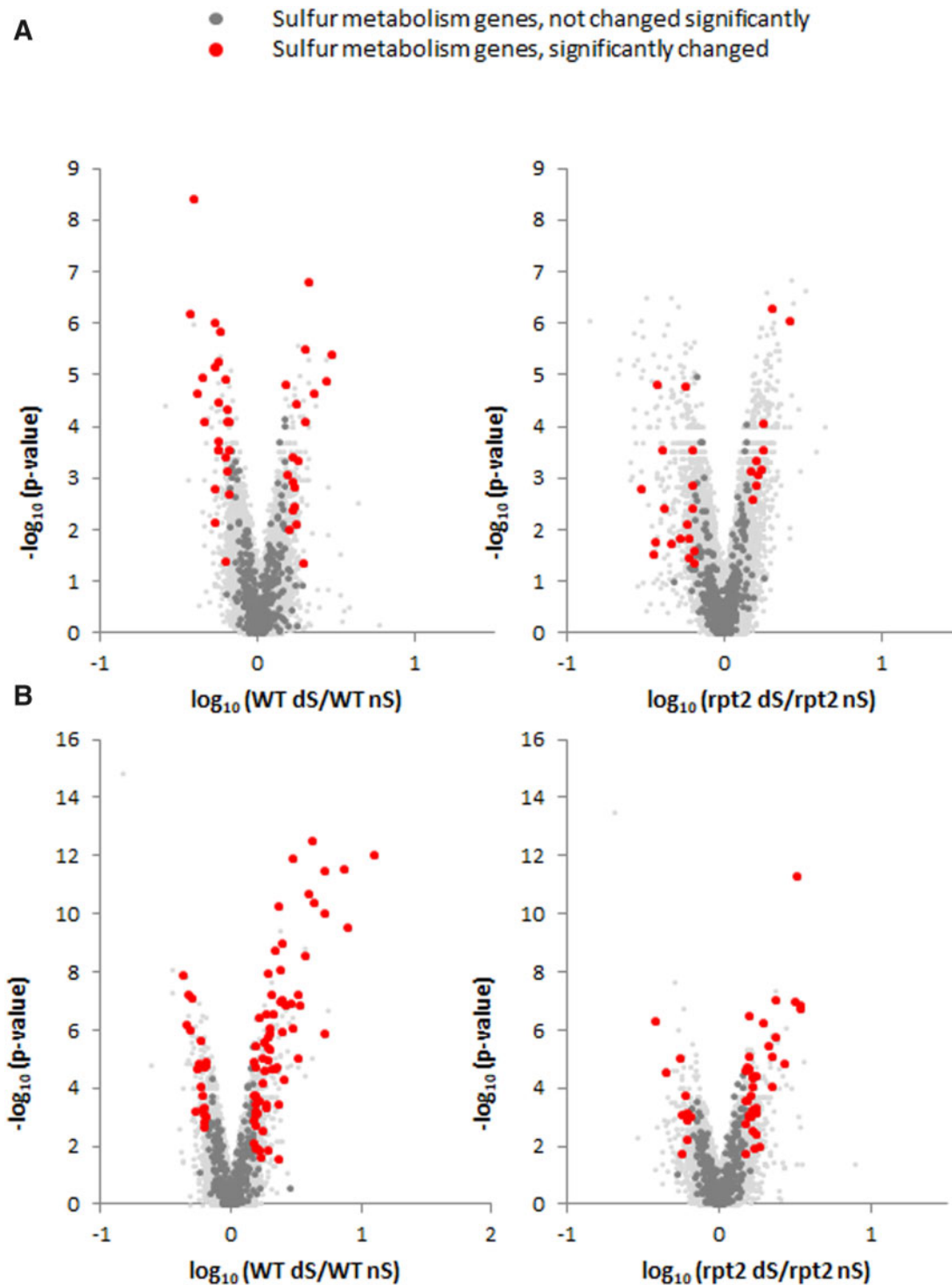


Fig. 4 Distribution of rosettes (A) and roots (B) transcripts based on the GO term 'sulfur metabolism'. On the left are volcano plots for the WT plants, and on the right for *rpt2a* mutant, both under S deficiency. Light gray dots represent all genes, while the specific GO category is represented by dark gray dots and black dots (significantly changed; fold change ≥ 1.5 and $P \leq 0.05$).

(**Supplementary Table S4**). We decided to verify the expression of six selected genes in the very same plant material by qRT-PCR, namely three genes from rosettes, *RING9* (At4g19700), *ATL13* (At4g30400) and *BTB1* (At5g67480), and three genes from roots, *FBS1* (At1g61340), *RING2* (At2g20030) and *PHD3* (At5g40590). All six genes encode E3 ligases from

different families. The data generally confirmed the results from microarrays (**Fig. 7**). The marker gene for S starvation conditions, *SDI1*, showed induction in roots of both genotypes but only for the WT rosettes, which confirmed our abovementioned observation that *rpt2a* mutant displays milder responses of genes belonging to the 'sulfur metabolism' GO category

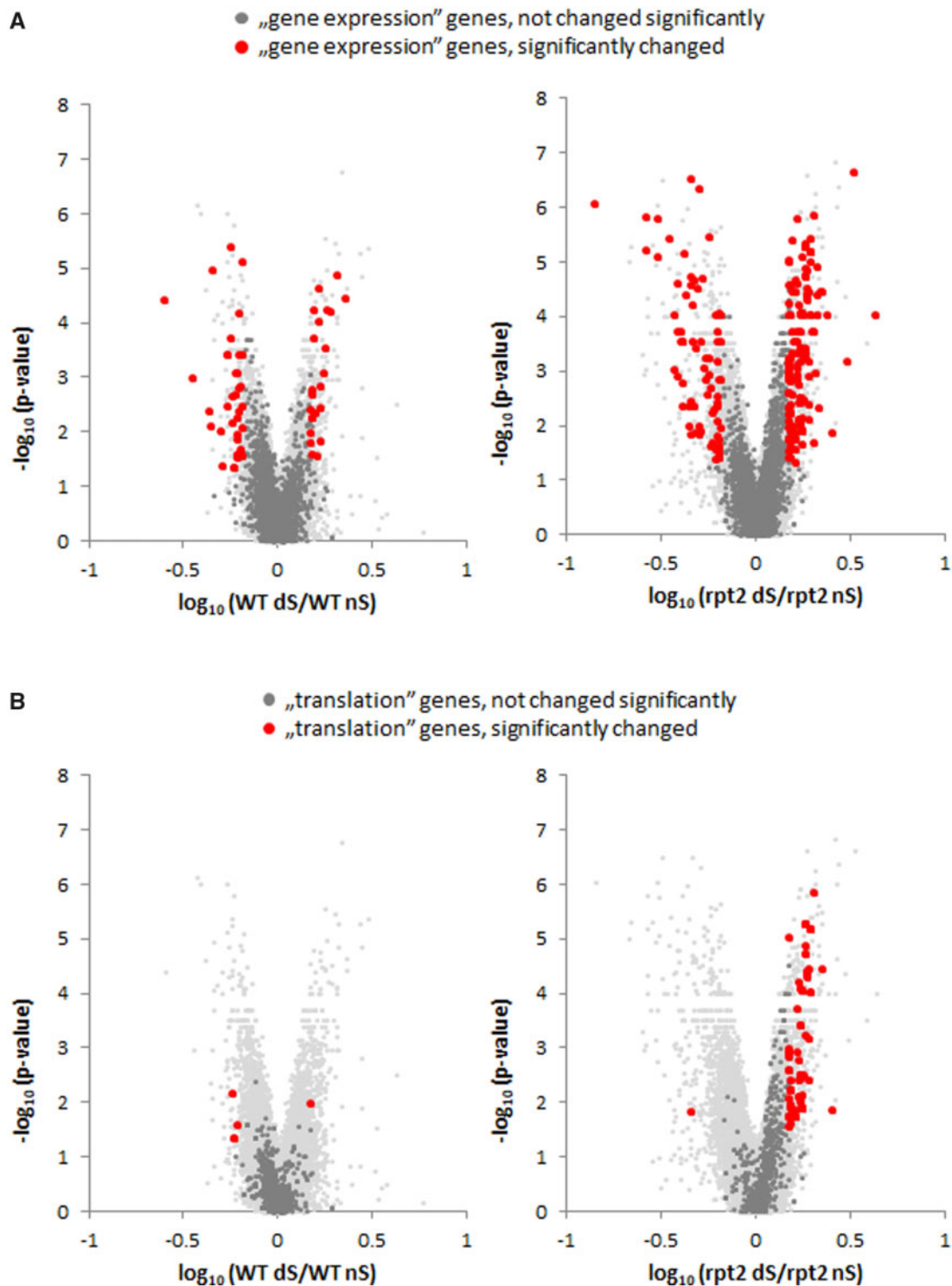


Fig. 5 Distribution of rosettes transcripts based on the GO term (A) 'translation' and (B) 'gene expression'. On the left are volcano plots for the WT plants, and on the right for *rpt2a* mutant, both under S deficiency. Light gray dots represent all genes, while the specific GO category is represented by dark gray dots and black dots (significantly changed; fold change ≥ 1.5 and $P \leq 0.05$).

(Fig. 4). The *BTB1*, *RING9* and *ATL13* showed differential expression only for the rosette tissue, and *RING2* is induced only in roots while *FBS1* and *PHD3* are regulated in both tissues.

Next, to see if the observed change of expression of selected genes encoding E3 ligases is general during S starvation we decided to look at their levels in 10-day-old S-starved seedlings

(Supplementary Fig. S10). Both, the WT and *rpt2a* seedlings grown in dS media demonstrated extensive upregulation of the *SDI1* gene, proving that the stress conditions were sensed. Almost all assayed genes showed similar patterns of differential expression in response to S starvation when compared to the mature plants.

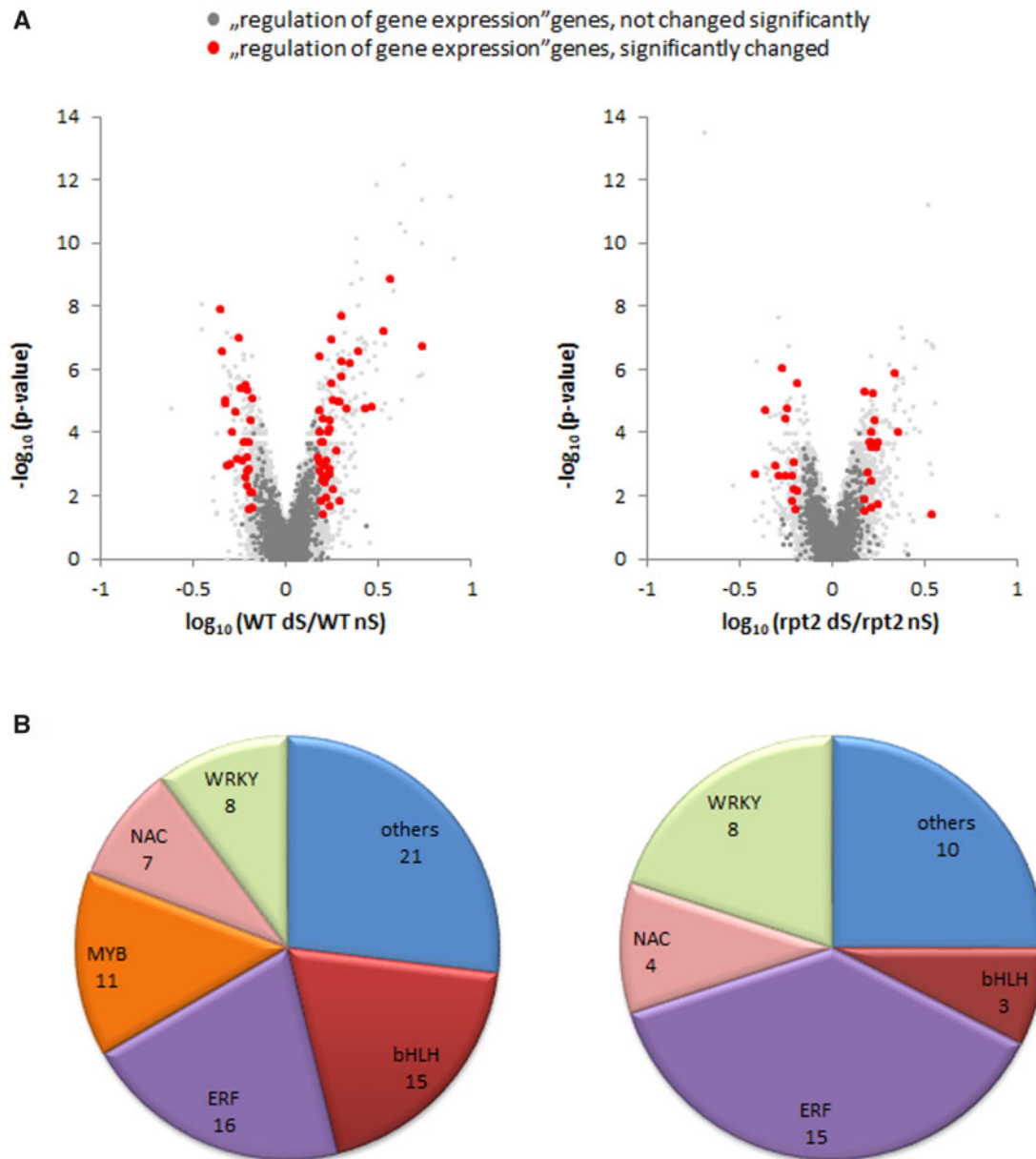


Fig. 6 (A) Distribution of root transcripts based on the GO term ‘regulation of gene expression’. On the left is a volcano plot for the WT plants, and on the right plot for *rpt2a* mutant, both under S deficiency. Light gray dots represent all genes, while specific GO category is represented by dark gray dots and black dots (significantly changed; fold change ≥ 1.5 and $P \leq 0.05$). (B) Pie charts show top TF families that contain the highest number of DEGs in the WT plants (left) and *rpt2a* mutant (right) roots.

Protein ubiquitination status is enhanced by S deficiency

To further investigate the effects of S deficiency on ubiquitin-dependent proteolysis, we compared the profiles of ubiquitin-conjugated proteins between the WT plants and *rpt2a* mutant in different tissues. Western blot analysis indicated that polyubiquitinated proteins were slightly more abundant in dS in both WT plants and *rpt2a* mutant though the statistically significant increase was indicated only for the latter (Fig. 8 and Supplementary Fig. S11). This effect was most apparent in the WT seedlings that were grown in dS conditions for longer periods (10 d) than the mature plants (5 d). In addition, there were more polyubiquitinated proteins

accumulated in the mutant seedlings compared to the WT plants under the nS conditions (Fig. 8 and Supplementary Fig. S11). This suggests that either ubiquitin-dependent 26S proteasome activity was inhibited, especially in the *rpt2a* mutant, or the protein ubiquitination system was activated under the dS conditions.

The level of transcriptional factor SLIM1 is controlled by the proteasome

To study the regulation and function of the major regulatory factor of S metabolism, SLIM1, we constructed transgenic Arabidopsis lines overexpressing either full-length protein (SLIM1_OX) or its C-terminal half [amino acids (aa): 286–567;

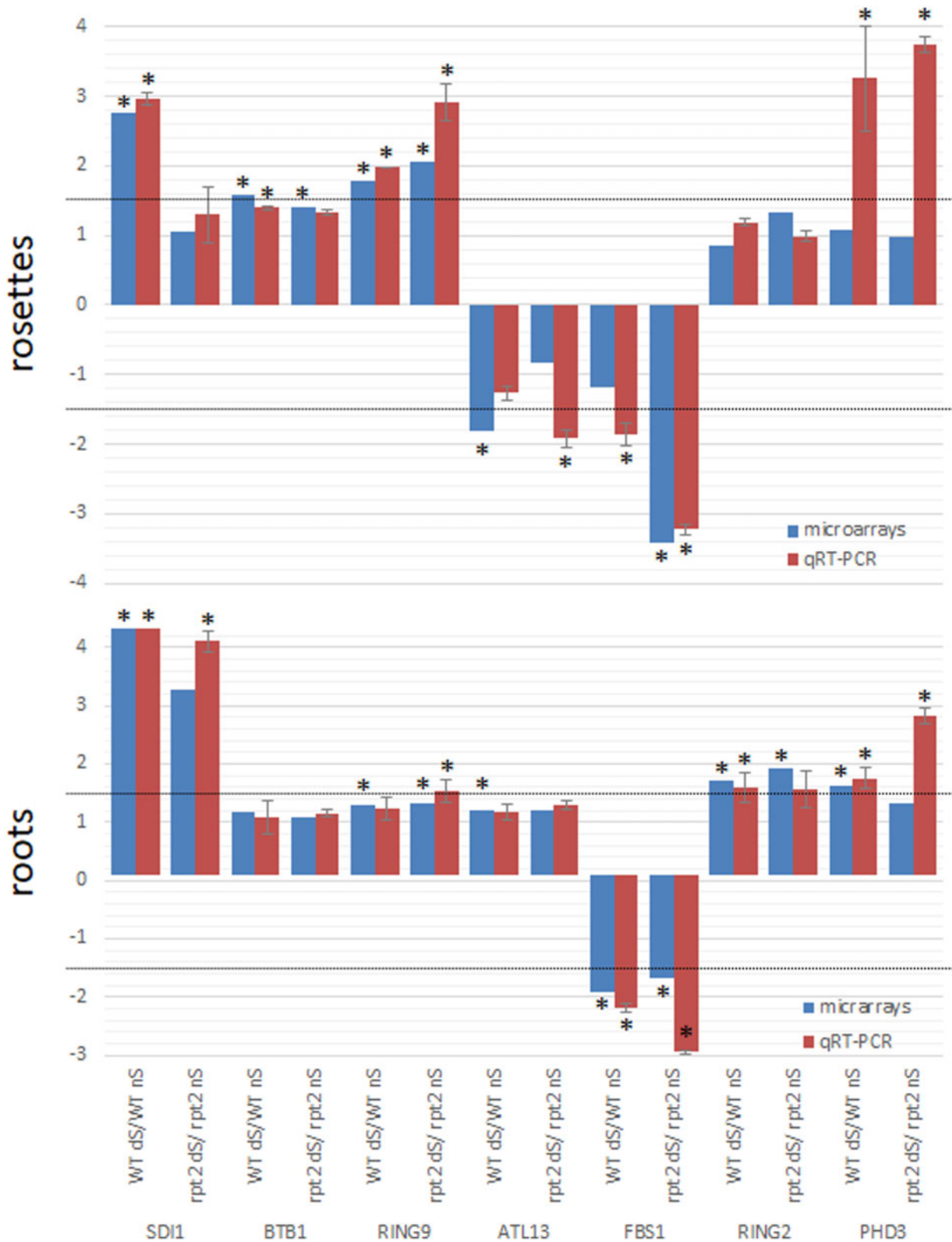


Fig. 7 Relative expression levels of the selected genes encoding E3 ubiquitin ligases in rosettes and roots of 5-week-old plants grown on dS media for 5 d analyzed by microarrays and validated by qRT-PCR. The Arabidopsis gene for Actin2 was used as an internal control to normalize the expression data and *SDI1* expression served to confirm S deficiency response. Bars represent mean fold change levels and SD assayed in dS-grown WT and *rpt2a* mutant plants in comparison with the expression of adequate Arabidopsis line grown in nS. Asterisks indicate significant differential expression ($P < 0.05$; three-way ANOVA for microarrays data and Student's *t*-test for qRT-PCR results). The black horizontal lines show the cutoff value of a 1.5-fold change. The expression level showed was averaged from three independent biological replicates, split into three technical replicates, each containing a pool of three to five plants.

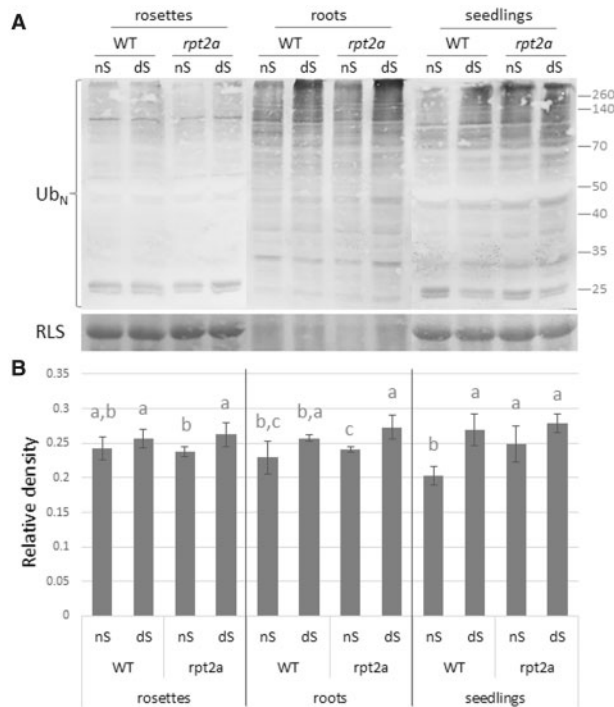


Fig. 8 Profiles of polyubiquitinated proteins in the WT plants and *rpt2a* mutant. (A) Equal amounts of protein extracts (35 μ g) were separated on SDS–PAGE, transferred to a membrane and probed with anti-polyubiquitin antibodies. Ub_N polyubiquitinated proteins. The Ponceau S-stained membrane showing the Rubisco large subunit is included as a loading control. The molecular weights (kDa) of the protein standards are shown on the right. The experiments were repeated three times with different biological replicates each time (**Supplementary Fig. S11**). (B) The graph showing the densitometric analysis, normalized against Ponceau staining of total proteins and are presented as the mean \pm standard deviation ($n = 3$). The significantly different samples ($P \leq 0.05$) are indicated with different letters for rosettes, roots and seedlings separately.

SLIM1-Ct_OX]. Both proteins fused at C-terminus to 10 \times c-Myc-tag were expressed under the control of the strong Cauliflower Mosaic Virus 35S promoter (35S), ensuring a high level of protein. However, we noticed that if we did not use the protein extracts from transgenic plants overexpressing full length immediately for western blot detection we could barely see the tagged protein after 12 h incubation at 4 $^{\circ}$ C (**Fig. 9A** and **Supplementary Fig. S12A**). This was not the case for the C-terminal part of SLIM1 that in contrary to full-length SLIM1 was not as quickly degraded after translation inhibition (**Fig. 9B** and **Supplementary Fig. S12B**). Moreover, we noticed the double band of the C-terminal part of SLIM1 protein suggesting the possibility of posttranslational modification, putatively ubiquitination. Thus, it was hypothesized that SLIM1 protein may be posttranslationally regulated and could be a target of ubiquitin-mediated proteolysis. To test this possibility, we treated the protein extracts from the plants overexpressing SLIM1 with a proteasome-specific inhibitor, MG132, and left it overnight. The abundance of the detected SLIM1 protein was the same as in the initial sample (**Fig. 9A** and **Supplementary Fig. S12A**). These results indicate that SLIM1 proteolysis is proteasome dependent.

Next, we wanted to check whether dS conditions affect the rate of SLIM1 protein degradation. To address this issue, we blocked translation elongation using cycloheximide (CHX) and compared the levels of SLIM1 protein in the seedlings grown for 11 d on either nS or dS. As shown in **Fig. 9B**, the levels of SLIM1 remained constitutively high in the presence or absence of S but decreased rapidly when treated with CHX, indicating that de novo protein synthesis is required for the observed SLIM1 protein accumulation. In conclusion, prolonged 11-day S starvation of plants did not have any protective effect on SLIM1 protein. However, in the shorter times of S starvation (2 d), SLIM1 was apparently degraded at a lower rate than after longer starvation (**Fig. 9C** and **Supplementary Fig. S12C**). Thus, we assume that, at the early stages of S deficiency, the constitutive degradation of SLIM1 protein is repressed.

The level of the close homolog of SLIM1, EIN3 protein, is controlled by specific signals like ethylene and others like glucose, light and phosphorylation (**Potuschak et al. 2003**, **Lee et al. 2006**, **Yoo et al. 2008**). We decided to check the effect of glucose and the ethylene biosynthetic precursor, 1-aminocyclopropane-1-carboxylic acid (ACC), on SLIM1 protein stability (**Fig. 9D** and **Supplementary Fig. S12D**). Unlike the effects observed for EIN3, where there was a positive correlation between the levels of EIN3 protein and ACC concentration, SLIM1 protein was not protected against degradation by the ACC treatment. On the other hand, it has been found that glucose can promote EIN3 degradation by an unknown mechanism, but we did not notice a similar effect on SLIM1 abundance. The level of transgenically overexpressed SLIM1 protein did not drop after treatments of the plants with glucose (**Fig. 9D** and **Supplementary Fig. S12D**).

SLIM1 interaction with F-box protein, EBF1

Because SLIM1 abundance is regulated by a proteasome-dependent pathway, we speculated that one or more specific E3 ubiquitin ligases would mediate the SLIM1 degradation process. Our attempts to find such a protein by means of co-immunoprecipitation and yeast two-hybrid screen of Arabidopsis cDNA library failed. The major challenge in using these strategies is that E3 ligase–substrate interactions are often too weak for successful co-purification of the target protein. We decided to use a targeted method, to determine whether the E3 ligases, EBF1 and EBF2, described to recognize EIN3 transcription factor, can also interact with other proteins of the EIL protein family. Yeast two-hybrid results clearly demonstrated the ability of EBF1 and EBF2 to recognize EIN3, EIL1 and EIL2, which is in agreement with literature data (**Potuschak et al. 2003**) (**Fig. 10**). Surprisingly, only EBF1 dimerizes with SLIM1 while EBF2 is unable to interact with SLIM1. EIL4 and EIL5 interact with neither EBF1 nor EBF2 (**Fig. 10**). The interaction region with EBF1 was further localized to the C-terminal part of SLIM1 (aa: 287–568), while its N-terminal part (aa: 1–286) cannot bind to this F-box protein (**Supplementary Fig. S13A**). The binding abilities between SLIM1 and EBF1 were further confirmed using the pull-down assay (**Fig. 10B**). We could not overexpress the full-length SLIM1 or C-terminal half of the SLIM1 protein in

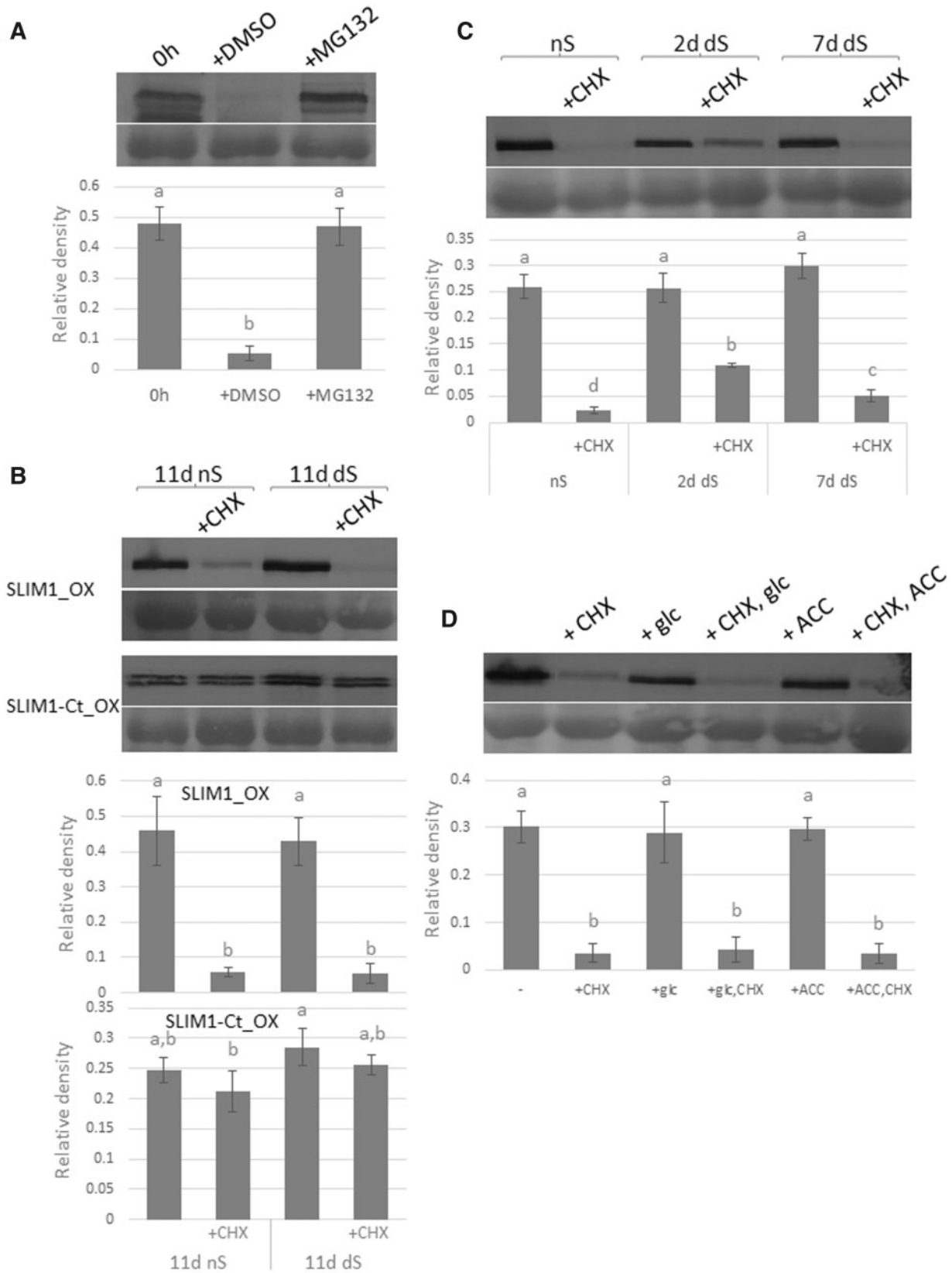


Fig. 9 SLIM1 protein is rapidly degraded through a proteasome-dependent pathway. (A) SLIM1 protein is stabilized by a specific proteasome inhibitor. Protein extracts from Arabidopsis 11-day-old SLIM1_OX seedlings were treated with mock (1% DMSO) or MG132 (50 μ M) for 12 h at 4°C before immunoblot assays (B) SLIM1 full-length protein is quickly degraded after translation inhibition. Arabidopsis 11-day-old SLIM1_OX and (continued)

Escherichia coli; therefore, the C-terminal half was further split into two equal parts: SLIM1_C1 (aa: 287–428) and SLIM1_C2 (aa: 418–568). The interaction with EBF1 was observed only for the SLIM1_C1 fragment (Fig. 10B).

Discussion

The aim of this study was to find the links connecting S metabolism with selective protein degradation. We report for the first time the involvement of the UPS-mediated degradation in the regulation of transcriptional response of Arabidopsis to S deficiency stress. It is also worth to underline that this is the first time that the transcriptomic analyses were done on rosettes and roots of mature plants subjected to short-time S starvation. All the existent microarray analyses were performed on Arabidopsis seedlings or mature plants kept in S deficiency conditions for at least 3 weeks (Watanabe and Hoefgen 2019). Different mechanisms might be responsible for transcriptional regulation during other developmental stages (e.g. mature plants versus seedlings) and different responses might be observed under various S starvation regimes. Our goal was to assay mainly the primary response to S deficiency and to exclude the secondary effects arising from the adaptive response; therefore, the stress was applied for a short time (5 d) yet sufficient to induce marker genes.

To enlighten the role of the proteasome during S starvation, we screened the transcriptional changes in *rpt2a* mutant challenged with S deficiency. Notably, rosettes of *rpt2a* mutant showed much more gene expression variability sharing a very small fraction of DEGs with the WT (8.6%). This might suggest that plants with proteasomal malfunction are overreacting to the stressful condition. On the contrary, in the category 'sulfur compound metabolic process', there were fewer genes and with expression changed to a lesser extent in the *rpt2a* mutant rosettes and roots. This proves the importance of proteasomal degradation processes during the response of Arabidopsis to S deficiency; the malfunction of the proteasome causes the delay of the reaction, which might lead to weaker adaptation of the plant to new S conditions.

During transcriptomic analyses, we found out that genes for snoRNA and pre-tRNA are significantly upregulated in *rpt2a* mutant rosettes. snoRNAs can be found in archaea as well as in eukaryotes and are involved in the chemical modification in nucleotides in RNA, mainly in ribosomal RNA in regions important for translation (Swiatowy and Jagodzinski 2018) and

necessary for the assembly of ribosomal subunits (Kressler et al. 2017). tRNA is responsible for the supply of free aa to the ribosomes for translation. The increased levels of both tRNAs and snoRNAs suggest the upregulation of ribosome biogenesis. Nonetheless, we did not observe the enhancement of total protein level in *rpt2a* mutant during S starvation (Supplementary Fig. S8). It was already verified that knockout mutation of the RPT2a gene did not alter global protein levels (Sako et al. 2012). However, mechanisms responsible for the observed upregulation of tRNA and snoRNA expressions under S deficiency and their link to proteasomal degradation remain unclear. The tRNA modulation represents a mechanism by which cells achieve altered expression of specific transcripts and proteins; however, we do not know whether such a mechanism was observed in this study. The physiological significance of variations in expression levels of individual tRNA genes is uncertain due to the large genetic redundancy of tRNA genes. This is especially true for variations in isodecoder gene sets (tRNAs having the same anticodon sequence), where no influence can be invoked on the use of codon during translation. Differences in isodecoder tRNA gene expression between different human samples do not lead to changes in the levels of mature tRNAs, but rather in a modification in the abundance of alternative products of the genes, such as tRNA degradation fragments that are linked to non-canonical biological functions unrelated to protein synthesis (Torres et al. 2019).

Only recently, with the development of next-generation sequencing, very small structures of ribonucleic acids (sRNA, 18–30 nucleotides long) were discovered. Initially, these molecules were thought to be a transient product of the degradation of tRNA, rRNA or snoRNA. Their wide occurrence in all living organisms suggests that they evolved early as one of the primary mechanisms of gene expression regulation (Babski et al. 2014). Increasing evidence suggests that sRNAs are important regulatory components in plant development and stress responses (Kamthan et al. 2015). Small tRNA-derived fragments (tRFs) are involved in the inhibition of protein synthesis and gene silencing either by targeting mRNA sequences or by competing with the original small RNAs for loading onto the RNA-induced silencing complex (RISC) (Wang et al. 2016). Interestingly, the generation of certain tRFs might be determined by tRNAs with amino acid specificity under different stress conditions or by distinct tissue types (Park and Kim 2018). The snoRNA-derived small RNAs (sdRNA) are the second most widely discussed class of noncoding RNA degradants. Recently, a functional analysis of sdRNAs revealed that they could have an miRNA-like function

Fig. 9 Continued

SLIM-Ct_OX seedlings grown on nS or dS media were supplemented with 100 μ M of CHX and incubated for 6 h before harvesting. (C) Short-term S deficiency stabilizes SLIM1 protein. Seven-day-old SLIM-OX seedlings were transferred to either nS or dS media for the indicated amounts of time and next supplemented with 100 μ M of CHX and incubated for 6 h before harvesting. (D) The effect of glucose or ACC on the stability of SLIM1. Arabidopsis 11-day-old SLIM1-OX seedlings grown on nS were supplemented with 100 μ M of CHX, 10 mM glucose, 10 μ M ACC or in combinations and incubated for 6 h before harvesting. The upper panel of each picture shows the result of Western blot probed with anti-Myc antibodies while the lower panel shows the amount of Rubisco Large Subunit protein used as a loading control stained with Ponceau S after transfer to the membrane. The experiments were repeated three to four times with different biological replicates each time (Supplementary Fig. S12). The graphs below the Western blots show the densitometric analysis, normalized against Ponceau staining of total proteins and are presented as the mean \pm standard deviation ($n = 3$). The significantly different samples ($P \leq 0.05$) are indicated with different letters.

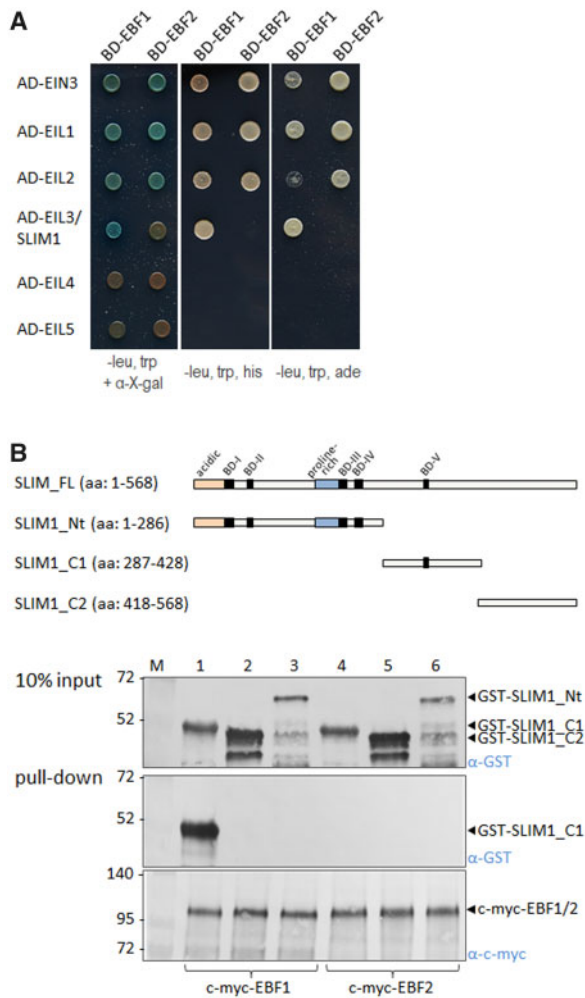


Fig. 10 Interactions between EBF1, EBF2 and EIL transcription factors. (A) Yeast two-hybrid experiment: yeast growth on selective plates lacking histidine, tryptophan and leucine (–leu, trp, his) or adenine, tryptophan and leucine (–leu, trp, ade) and on control plates lacking only tryptophan and leucine (–trp, –leu) is shown. The fusion proteins are indicated. The plates were photographed after 3 d at 30°C. (B) Pull-down assays using GST and c-myc-tagged proteins expressed in *E. coli*. In the upper part is a schematic representation of the SLIM1 protein regions used in the pull-down experiment; SLIM1_FL—full-length SLIM1 protein with domains characteristic for EIL protein family: ‘acidic’, N-terminal region rich in acidic aa; BD, basic domain rich in basic aa; proline-rich, region rich in prolines; aa, amino acids. Precipitated proteins were detected by immunoblots. Input shows the presence of the GST-tagged proteins in crude extracts. After affinity purification through the anti-c-myc gel with attached EBF1 or EBF2, only the GST-tagged protein in lane 1 (SLIM1_C1) is detected due to interaction. There is no interaction detected between EBF1 and SLIM1_C2 or SLIM1_Nt (lane 2 and 3). The negative controls resents the lack of interaction between EBF2 with SLIM1_C1, SLIM1_C2 or SLIM1_Nt are shown in lanes 4, 5 and 6. The molecular marker (M) with the size (kDa) of the proteins is indicated. Expected sizes of the fusion proteins: c-myc-EBF1—96 kDa, c-myc-EBF2—96 kDa, c-myc-SLIM1_C1—44 kDa, GST-SLIM1_C2—42 kDa and GST-SLIM1_Nt—59 kDa.

but could also affect the alternative splicing of mRNAs (Wang et al. 2016). In reaction to stress, RNA metabolism is an important element of translational repression and splice site changes. In *Arabidopsis* and barley, tRFs have been shown to be involved

in the phosphate deficiency and drought stress responses, while heat and osmotic stresses induce sdRNA in wheat (Wang et al. 2016). Under the dS conditions of our experiment, *Arabidopsis* rosettes of *rpt2a* mutant showed upregulation of 57 out of 71 snoRNAs assigned in the TAIR10 *Arabidopsis* genome release. We do not know whether these snoRNAs undergo degradation together with induced pre-tRNAs. By switching from functional tRNAs and snoRNAs for enhancing translation into inhibitory tRFs and sdRNAs for the suppression of normal metabolism, these molecules might provide a sequence-specific tool for fine-tuning the gene expression in response to S deficiency stress conditions. By immediately reducing gene expression using tRFs and sdRNAs, plants can minimize unwanted cellular responses and improve survival under stress. It is tempting to speculate that, in the conditions of S deficiency stress and proteasomal malfunction where the proteins to be removed cannot be efficiently degraded, plants turn on the rescue mechanism to reduce the level of these proteins through posttranscriptional regulation. Future research that identifies if tRF and sdRNA formations are actually induced during S deficiency stress and what the target genes are will lead to a better understanding of the regulatory mechanisms.

Analysis of GO term enrichment demonstrated that in the WT roots, the ‘regulation of gene expression’ containing mostly transcription factor genes is specifically enhanced. Only half of the DEGs encoding transcription factors were regulated in the *rpt2a* mutant with none of the MYB family comparing to 11 MYBs changed in the WT, mostly belonging to the R2R3 type that is only present in plants (Stracke et al. 2001). Several R2R3 MYB family transcription factors have been identified as positive or negative regulators of indole glucosinolates synthesis/degradation that are secondary S-containing metabolites found in the Brassicaceae family (Watanabe and Hoefgen 2019). The backbone of glucosinolates contains three S atoms, which can account for up to 30% of the total S content of the entire plant; therefore, it is not surprising that in the situation of S deficiency, their contents might need to be tightly regulated (Falk et al. 2007). In the WT plants, two of the MYBs suggested to be associated with S metabolism are downregulated, namely MYB51 and MYB76. Proteasomal malfunction and possibly ubiquitin-mediated degradation might then affect glucosinolates metabolism.

We identified several E3 ligases with genes showing changed expression due to S deficiency. The altered levels of transcript of six selected genes from different E3 ligase families, namely RING9 (At4g19700); ATL13 (At4g30400); BTB1 (At5g67480); FBS1 (At1g61340); RING2 (At2g20030); and PHD3 (At5g40590), were validated in different tissues and stages of plant growth. Surprisingly, FBS1 was strongly induced in seedlings, while it was repressed in rosettes and roots of 5-week-old plants. PHD3 did not respond to S starvation in the seedlings, suggesting that it may play a role in other developmental stages of plants. Finding the proteins that are targeted by these E3 ligases will be the subject of future research. So far, only a few E3 ligases have been associated with response to certain biotic and abiotic stresses (Xu and Xue 2019).

Comparison of the profiles of ubiquitin-conjugated proteins between the WT plants and *rpt2a* mutant in different tissues

indicated that polyubiquitinated proteins were vaguely more abundant in dS in both WT plants and *rpt2a* mutant. This indicates that ubiquitin-dependent 26S proteasome activity was suppressed under the dS conditions. It has been found that the upregulation of 26S proteasome subunit genes reflects a decrease in its activity in plants (Kurepa et al. 2008, Sakamoto et al. 2011). The fact that proteasomal activity is inhibited in dS conditions and in *rpt2a* mutant suggests the possible existence of specific unknown substrates degraded through this proteolytic pathway in response to S deficiency and specifically processed through RPT2A. During zinc deficiency, RPT2A and RPT5A have been shown to be upregulated, but their paralogs RPT2B and RPT5B were not, indicating that the involvement of a certain subunit might be stress specific (Sakamoto et al. 2011). It is suggested that different proteasome subunits may play distinct and specific roles in environmental stress tolerance (Xu and Xue 2019). Although we did not find any significant changes in the expression of RPT genes in 5-week-old plants maintained in dS conditions for 5 d, we cannot exclude that they directly interact with certain elements of S metabolism, such as SLIM1. In future experiments, we are planning to check whether the degradation of SLIM1 is mediated by RPT2a or any other RPTs.

SLIM1 can interact with E3 ligase EBF1 but not with EBF2. EBF1 and EBF2 share a 57% identity in amino acid sequence (Guo and Ecker 2003), and each contains a well-conserved F-box motif at the N-terminus and 18 tandem leucine-rich repeats (LRRs) in the C-terminus. LRR domains from both proteins were enough to interact with EIN3 protein in yeast two-hybrid assays (Guo and Ecker 2003). Interestingly, it was also demonstrated that the C-terminus of EIN3 is necessary for the interaction, while the C-terminal part is highly divergent in the EIL protein family, sharing only a 24% identity with SLIM1. However, the interaction region with EBF1 is also located in the C-terminal part of SLIM1. The results of the pull-down locate it further to aa 287–428 (Fig. 10B). Interestingly, alignment of the amino acid sequences of the three so far described proteins able to interact with EBF1, namely EIN3, EIL1 and PIF3 (Potuschak et al. 2003, Jiang et al. 2017), with SLIM1 amino acid sequence shows several conserved residues mapping to the fragment proved to interact with EBF1 (Supplementary Fig. S13B). That motif could be potentially recognized by EBF1. Though EBF1 clearly interacts with the C-terminal fragment of SLIM1, it does not lead to its degradation (Fig. 9B). This might suggest that the lysine(s) to be ubiquitinated therefore marking SLIM1 for degradation are located out of the C-terminal region. We did not test whether the interaction of EBF1 with SLIM1 was responsible for the quick degradation of the latter protein and whether it was influenced by the S nutritional status; however, it will be the matter of the future experiments. It is especially interesting because EIN3 and SLIM1 can form heterodimers to out-compete SLIM1 from its targeted DNA-binding sites (Wawrzyńska and Sirko 2016). The ability of both proteins to interact with EBF1 adds yet another layer of regulation.

Conclusions

The impact of ubiquitin-mediated protein degradation determines many aspects of the response to external and internal

stimuli in plants. UPS degradation is critical for the rapid inhibition of target protein activity, such as transcription factors, and the rapid release or activation of downstream targets, such as protein repressors. We presented and discussed novel findings on the regulation of S metabolism through proteasomal degradation. Though it is a challenge to fully characterize the UPS and its substrates for their diverse role in S metabolism, resolving these regulation mechanisms will pave the way to improve S acquisition and utilization efficiency in crops.

Materials and Methods

Plant material and growth conditions

Wild-type *A. thaliana* and all employed mutant lines were of the Columbia-0 (Col-0) ecotype. The T-DNA insertion mutants, such as *rpt2a-3*, *rpn10-1* and *rpn12a-1*, were a kind gift of J. Smalle (Kurepa et al. 2009). Transgenic lines overexpressing full-length SLIM1 or C-terminal half of the SLIM1 protein were obtained by the *Agrobacterium tumefaciens*-mediated floral dip method (Clough and Bent 1998). For most assays, seeds were surface-sterilized (Zientara et al. 2009), exposed to 4°C in the dark for 3 d and then germinated on 0.7% agar containing half-strength Hoagland's medium (Schat et al. 1996). Two types of media were used in the experiments that contained either normal sulfur supply ('nS'; 1 mM sulfate) or sulfur deficient ('dS'; 10 μM sulfate). Seedlings were grown under a 12/12-h light/dark cycle at a temperature of 22°C. For drug treatments, seedling protein extracts were treated with MG132 (50 μM), or dimethyl sulfoxide (DMSO; 1%) for 12 h at 4°C. Alternatively, seedlings were incubated in the presence of CHX (100 μM), glucose (10 mM) or ACC (10 μM). All chemicals were supplied by Sigma-Aldrich (St. Louis, MI, USA). Plant material for transcriptomic analyses was grown in Arapronics' boxes (Arapronics, Liège, Belgium) kept under an 8/16-h light/dark cycle at a temperature of 22°C (light intensity 157.67 ± 19.78 μE m⁻² s⁻¹; 16 plants/box) for 5 weeks, with weekly changes in the medium. Before harvesting, plants were kept either in the same media (nS) or S starved for 5 d in dS media.

Gene cloning and plasmid construction

Standard techniques were used for DNA restriction/ligation manipulation and *E. coli* transformation (Green et al. 2012); all enzymes were from Thermo Fisher Scientific (Waltham, MA, USA). Gateway BP and LR recombination reactions were performed as described in the manufacturer's protocols using original plasmids (pENTR/D-TOPO, pDEST22, pDEST32) and enzymes (Thermo Fisher Scientific). For the transgenic plant construction, entry clones encoding full-length SLIM1 (aa: 1–568) and SLIM-Ct truncated protein (aa: 287–568) were recombined into binary vector pGWB420 (Nakagawa et al. 2007, RRID: Addgene_74814). All plasmid constructions were verified by DNA sequencing. Primers used for amplification and appropriate constructs obtained after cloning are listed in Supplementary Table S1.

Yeast two-hybrid (Y2H) assay

Manipulation of yeast cells and protein interaction screening were performed according to standard protocols (Clontech Yeast Protocol Handbook, PT3024-1). The Y2HGold strain of *Saccharomyces cerevisiae* (Takara Bio USA, Inc., Mountain View, CA) was used for transformation, and the protein interactions in Y2H were confirmed for their ability to activate the reporter genes *HIS3* or *ADE2* in triplicate (three independently transformed yeast colonies).

Gene expression analysis

Total RNA was isolated from seedlings using TRI Reagent[®] (Molecular Research Center, Cincinnati, OH, USA) according to the manufacturer's protocol (Chomczynski and Sacchi 1987). For the qRT-PCR analysis, 2 μg of RNA was reverse-transcribed using a Maxima First Strand cDNA Synthesis Kit (Thermo Fisher Scientific) according to the manufacturer's instructions. As a template for qRT-PCR, the 100 times dilutions of synthesized cDNA were used. The qRT-PCR was performed in a PikoReal[™] Real-Time PCR System (Thermo Scientific, Lithuania). The gene encoding actin 2 (At3g18780) was selected as an internal

control to normalize the quantity of total RNA present in each sample. All the primers used for qRT-PCR are listed in [Supplementary Table S2](#). The specificity of the forward and reverse primers to the candidate gene was checked using the NCBI-BLAST website (<http://www.ncbi.nlm.nih.gov/blast/Blast.cgi> (June 16, 2020, date last accessed), RRID: SCR_004870) and melting curve analysis following qRT-PCR. The reaction mixture (6 μ l) contained 3 μ l of DyNAmo Color Flash SYBR Green Master Mix (Thermo Fisher Scientific), 0.6 μ M each of forward and reverse primers and 1 μ l of cDNA template. The qRT-PCR was carried out in triplicate (technical repeats) of three biological repeats to ensure the reproducibility of the results. Relative gene expression levels were calculated using the delta-delta Ct method (Livak and Schmittgen 2001) as the transcription level under dS stress treatment compared to the transcription level in control conditions (nS). Statistical differences were analyzed using Student's *t*-test.

Microarray analysis

For the microarray analysis, hydroponically grown 5-week-old WT and *rpt2a* plants were transferred to dS media for 5 d. Three biological (each consisting of 4–5 plants) replicates per genotype and treatment were collected and divided into rosettes and roots. RNA was isolated from stressed and control plants using Direct-zol RNA MiniPrep kit (Zymo Research, Irvine, CA, USA) and digested with TURBOTM DNase (Thermo Fisher Scientific). Microarray expression analysis was performed using the Affymetrix Gene Atlas system according to the manufacturer's instructions. A mass of 100 ng of total RNA that passed an initial quality control screen was prepared for the Affymetrix whole-transcriptome microarray analysis using the Ambion WT Expression Kit (4411973). The resulting sense-strand cDNA was fragmented and labeled using the Affymetrix GeneChip[®] WT Terminal Labeling Kit (part no. 900671). Labeled samples were hybridized to the Arabidopsis Gene 1.1 ST Array Strip (Affymetrix, Santa Clara, CA, USA). The microarrays were then scanned with an Affymetrix GeneAtlas scanner, and the intensity signals for each of the probe sets were written by Affymetrix software into CEL files. The CEL files were imported into the Transcriptome Analysis Console Software 4.0 (Thermo Fisher Scientific, USA) with the use of robust multi-array averaging. During this step, background correction was applied based on the global distribution of the perfect match probe intensities and the affinity for each of the probes (based on their sequences) was calculated. In addition, the probe intensities were quantile normalized (Bolstad et al. 2003) and log₂-transformed and the median polish summarization was applied to each of the probe sets. Qualitative analysis was then performed (e.g. principal components analysis) to identify outliers and artifacts on the microarray. The microarray data have been deposited in Gene Expression Omnibus (<https://www.ncbi.nlm.nih.gov/geo/> (June 16, 2020, date last accessed), RRID: SCR_005012) and are accessible through GEO Series accession number GSE 137728.

Immunoblot analyses

For protein isolation, seedlings were homogenized in 100 μ l of extraction buffer (50 mM Tris-HCl, pH 7.5) with 1 μ l of Protein Inhibitor Cocktail (Sigma-Aldrich) and centrifuged at 13,000 rpm for 5 min at 4°C. Proteasome inhibitor MG132 (1 μ l from 5 mM stock, Sigma-Aldrich) or DMSO was added, if indicated, and samples were kept at 4°C for 12 h. Proteins were separated on 10% SDS-polyacrylamide gels, transferred to the nitrocellulose membrane (Bio-Rad, Hercules, CA, USA) and visualized by staining with Ponceau S. Membranes were blocked with 5% nonfat dry milk and then probed with either mouse anti-c-Myc monoclonal IgG (Santa Cruz Biotechnology, Santa Cruz, CA, USA Cat # sc-40, RRID: AB_627268) for tagged SLIM1 detection or anti-UBQ11 polyclonal IgG (AgriSera, Vännäs, Sweden Cat # AS08 307, RRID: AB_2256904). Goat anti-mouse IgG (Sigma-Aldrich Cat # A3562, RRID: AB_258091) or goat anti-rabbit (Sigma-Aldrich Cat # A3687, RRID: AB_258103) coupled to alkaline phosphatase was used as a secondary antibody. Proteins were visualized by adding 5 ml of 5-bromo-4-chloro-3-indolyl phosphate/nitro blue tetrazolium solution (BioShop, Burlington, Ontario, Canada) at room temperature. The band intensities of the protein of interest were quantified using ImageJ (NIH, Bethesda, MD, USA), and the densitometric values were normalized against Ponceau staining of the membrane. Next, they were analyzed using normalization where data points are divided by the sum of all data points in a replicate (Normalization by Sum of all Data Points in a Replicate; Degasperis et al. 2014). The statistical significance

was tested by one-way analysis of variance (ANOVA) and Fisher's Least Significant Difference (LSD) post hoc test.

Pull-down assay

The plasmids encoding the N-terminal Glutathione S-transferase (GST) or c-myc tag linked to the proteins being investigated are listed in [Supplementary Table S1](#). All GST- and c-myc-tagged proteins were expressed in *E. coli* Rosetta (DE3). Total proteins containing c-myc fusion proteins (EBF1 or EBF2) were extracted from bacteria by sonication in Radioimmunoprecipitation assay buffer (RIPA buffer; Thermo Fisher Scientific) supplemented with Protease Inhibitor Cocktail (Sigma-Aldrich) and purified on EZviewTM Red Anti-c-myc Affinity Gel (Sigma-Aldrich) according to the manufacturer's protocol. Next, the crude extracts containing GST fusion proteins [SLIM1_C1 (aa: 287–428), SLIM1_C2 (aa: 418–568) or SLIM1_Nt (aa: 1–286)] were incubated with above-prepared raisins at 4°C overnight with gentle rocking. The raisins were washed six times with RIPA buffer, boiled with 2 \times SDS-PAGE gel loading buffer, subjected to SDS-PAGE and next immunoblotted using mouse monoclonal anti-GST IgG and anti-c-myc IgG (Sigma-Aldrich, G1160 and Santa Cruz Biotechnology Inc., SC-40) as primary antibody and anti-mouse IgG conjugated to alkaline phosphatase (Sigma-Aldrich, A3562) as a secondary antibody.

Bioinformatic tools

After the quality checks of microarray data, the three-way ANOVA model using the method of moments (Eisenhart 1947) was applied, which permitted the creation of lists of genes that were significantly and differentially expressed between the biological variants (cutoff values: *P*-value \leq 0.05, fold change \geq 1.5). The function was ascribed to the obtained lists of genes using the agriGO v2.0 analysis tool (Tian et al. 2017) (<http://systemsbiology.cau.edu.cn/agriGOv2> (June 16, 2020, date last accessed), RRID: SCR_0069890) with TAIR10_2017 background and Plant GO Slim list of GO terms. The heat maps were drawn using the Network Analysis Tools (NeAT) webpage (http://rsat.sb-roscoff.fr/draw_heatmap_form.php (June 16, 2020, date last accessed)).

Supplementary Data

Supplementary data are available at PCP online.

Funding

The National Science Centre in Poland [grant Opus no 2014/15/B/NZ1/01887].

Acknowledgments

We thank Prof. Jan Smalle for sharing the proteasomal mutants seeds. The transcriptomic analyses were conducted at the Laboratory of Microarrays Analyses in IBB PAS. We are grateful to all members of our laboratory for stimulating discussions.

Disclosures

The authors have no conflicts of interest to declare.

References

- Arabi, F., Kusajima, M., Tohge, T., Konishi, T., Gigolashvili, T., Takamune, M., et al. (2016) Sulfur deficiency-induced repressor proteins optimize glucosinolate biosynthesis in plants. *Sci. Adv.* 2: e1601087.
- Babski, J., Maier, L.K., Heyer, R., Jaschinski, K., Prasse, D., Jäger, D., et al. (2014) Small regulatory RNAs in Archaea. *RNA Biol.* 11: 484–493.
- Binder, B.M., Walker, J.M., Gagne, J.M., Emborg, T.J., Hemmann, G., Bleecker, A.B., et al. (2007) The Arabidopsis EIN3 binding F-box proteins EBF1 and

- EBF2 have distinct but overlapping roles in ethylene signaling. *Plant Cell* 19: 509–523.
- Bolstad, B.M., Irizarry, R.A., Astrand, M. and Speed, T.P. (2003) A comparison of normalization methods for high density oligonucleotide array data based on variance and bias. *Bioinformatics* 19: 185–193.
- Chao, Q., Rothenberg, M., Solano, R., Roman, G., Terzaghi, W. and Ecker, J.R. (1997) Activation of the ethylene gas response pathway in Arabidopsis by the nuclear protein ETHYLENE-INSENSITIVE3 and related proteins. *Cell* 89: 1133–1144.
- Chomczynski, P. and Sacchi, N. (1987) Single-step method of RNA isolation by acid guanidinium thiocyanate-phenol-chloroform extraction. *Anal. Biochem.* 162: 156–159.
- Clough, S.J. and Bent, A.F. (1998) Floral dip: a simplified method for *Agrobacterium*-mediated transformation of *Arabidopsis thaliana*. *Plant J.* 16: 735–743.
- Degasperi, A., Birtwistle, M.R., Volinsky, N., Rauch, J., Kolch, W. and Kholodenko, B.N. (2014) Evaluating strategies to normalise biological replicates of Western blot data. *PLoS One* 9: e87293.
- Des Marais, D.L. and Juenger, T.E. (2010) Pleiotropy, plasticity, and the evolution of plant abiotic stress tolerance. *Ann. N Y Acad. Sci.* 1206: 56–79.
- Eisenhart, C. (1947) The assumptions underlying the analysis of variance. *Biometrics* 3: 1–21.
- Falk, K.L., Tokuhisa, J.G. and Gershenzon, J. (2007) The effect of sulfur nutrition on plant glucosinolate content: physiology and molecular mechanisms. *Plant Biol. (Stuttg)* 9: 573–581.
- Gagne, J.M., Smalle, J., Gingerich, D.J., Walker, J.M., Yoo, S.D., Yanagisawa, S., et al. (2004) Arabidopsis EIN3-binding F-box 1 and 2 form ubiquitin-protein ligases that repress ethylene action and promote growth by directing EIN3 degradation. *Proc. Natl. Acad. Sci. USA* 101: 6803–6808.
- Genschik, P., Parmentier, Y., Durr, A., Marbach, J., Criqui, M.C., Jamet, E., et al. (1992) Ubiquitin genes are differentially regulated in protoplast-derived cultures of *Nicotiana sylvestris* and in response to various stresses. *Plant Mol. Biol.* 20: 897–910.
- Green, M.R., Sambrook, J. and Sambrook, J. (2012) *Molecular Cloning: A Laboratory Manual*. Cold Spring Harbor Laboratory Press, Cold Spring Harbor, NY.
- Guo, H. and Ecker, J.R. (2003) Plant responses to ethylene gas are mediated by SCF (EBF1/EBF2)-dependent proteolysis of EIN3 transcription factor. *Cell* 115: 667–677.
- Guo, H. and Ecker, J.R. (2004) The ethylene signaling pathway: new insights. *Curr. Opin. Plant Biol.* 7: 40–49.
- Hua, Z.H. and Vierstra, R.D. (2011) The Cullin-RING ubiquitin-protein ligases. *Annu. Rev. Plant Biol.* 62: 299–334.
- Jiang, B.C., Shi, Y.T., Zhang, X.Y., Xin, X.Y., Qi, L.J., Guo, H.W., et al. (2017) PIF3 is a negative regulator of the CBF pathway and freezing tolerance in Arabidopsis. *Proc. Natl. Acad. Sci. USA* 114: E6695–E6702.
- Kamthan, A., Chaudhuri, A., Kamthan, M. and Datta, A. (2015) Small RNAs in plants: recent development and application for crop improvement. *Front. Plant Sci.* 6: 208.
- Kohler, A., Cascio, P., Leggett, D.S., Woo, K.M., Goldberg, A.L. and Finley, D. (2001) The axial channel of the proteasome core particle is gated by the Rpt2 ATPase and controls both substrate entry and product release. *Mol. Cell* 7: 1143–1152.
- Komander, D. and Rape, M. (2012) The ubiquitin code. *Annu. Rev. Biochem.* 81: 203–229.
- Kressler, D., Hurt, E. and Baßler, J. (2017) A puzzle of life: crafting ribosomal subunits. *Trends Biochem. Sci.* 42: 640–654.
- Kurepa, J., Toh, E.A. and Smalle, J.A. (2008) 26S proteasome regulatory particle mutants have increased oxidative stress tolerance. *Plant J.* 53: 102–114.
- Kurepa, J., Wang, S., Li, Y., Zaitlin, D., Pierce, A.J. and Smalle, J.A. (2009) Loss of 26S proteasome function leads to increased cell size and decreased cell number in Arabidopsis shoot organs. *Plant Physiol.* 150: 178–189.
- Lee, J.H., Deng, X.W. and Kim, W.T. (2006) Possible role of light in the maintenance of EIN3/EIL1 stability in Arabidopsis seedlings. *Biochem. Biophys. Res. Commun.* 350: 484–491.
- Lin, W.Y., Huang, T.K. and Chiou, T.J. (2013) NITROGEN LIMITATION ADAPTATION, a target of microRNA827, mediates degradation of plasma membrane-localized phosphate transporters to maintain phosphate homeostasis in Arabidopsis. *Plant Cell* 25: 4061–4074.
- Lingam, S., Mohrbacher, J., Brumbarova, T., Potuschak, T., Fink-Straube, C., Blondet, E., et al. (2011) Interaction between the bHLH transcription factor FIT and ETHYLENE INSENSITIVE3/ETHYLENE INSENSITIVE3-LIKE1 reveals molecular linkage between the regulation of iron acquisition and ethylene signaling in Arabidopsis. *Plant Cell* 23: 1815–1829.
- Liu, T.Y., Huang, T.K., Tseng, C.Y., Lai, Y.S., Lin, S.I., Lin, W.Y., et al. (2012) PHO2-dependent degradation of PHO1 modulates phosphate homeostasis in Arabidopsis. *Plant Cell* 24: 2168–2183.
- Livak, K.J. and Schmittgen, T.D. (2001) Analysis of relative gene expression data using real-time quantitative PCR and the 2^{-ΔΔC_T} method. *Methods* 25: 402–408.
- Long, T.A., Tsukagoshi, H., Busch, W., Lahner, B., Salt, D.E. and Benfey, P.N. (2010) The bHLH transcription factor POPEYE regulates response to iron deficiency in Arabidopsis roots. *Plant Cell* 22: 2219–2236.
- Lyzenga, W.J. and Stone, S.L. (2012) Abiotic stress tolerance mediated by protein ubiquitination. *J. Exp. Bot.* 63: 599–616.
- Maruyama-Nakashita, A., Nakamura, Y., Tohge, T., Saito, K. and Takahashi, H. (2006) Arabidopsis SLIM1 is a central transcriptional regulator of plant sulfur response and metabolism. *Plant Cell* 18: 3235–3251.
- Mazzucotelli, E., Belloni, S., Marone, D., De Leonardi, A.M., Guerra, D., Fonzo, N., et al. (2006) The E3 ubiquitin ligase gene family in plants: regulation by degradation. *Curr. Genomics* 7: 509–522.
- Nakagawa, T., Suzuki, T., Murata, S., Nakamura, S., Hino, T., Maeo, K., et al. (2007) Improved Gateway binary vectors: high-performance vectors for creation of fusion constructs in transgenic analysis of plants. *Biosci. Biotechnol. Biochem.* 71: 2095–2100.
- Pan, W.B., Wu, Y.R. and Xie, Q. (2019) Regulation of ubiquitination is central to the phosphate starvation response. *Trends Plant Sci.* 24: 755–769.
- Park, E.J. and Kim, T.H. (2018) Fine-tuning of gene expression by tRNA-derived fragments during abiotic stress signal transduction. *Int. J. Mol. Sci.* 19: 518.
- Peng, M.S., Hannam, C., Gu, H.L., Bi, Y.M. and Rothstein, S.J. (2007) A mutation in NLA, which encodes a RING-type ubiquitin ligase, disrupts the adaptability of Arabidopsis to nitrogen limitation. *Plant J.* 50: 320–337.
- Pickart, C.M. and Cohen, R.E. (2004) Proteasomes and their kin: proteases in the machine age. *Nat. Rev. Mol. Cell Biol.* 5: 177–187.
- Potuschak, T., Lechner, E., Parmentier, Y., Yanagisawa, S., Grava, S., Koncz, C., et al. (2003) EIN3-dependent regulation of plant ethylene hormone signaling by two Arabidopsis F box proteins: EBF1 and EBF2. *Cell* 115: 679–689.
- Pratelli, R., Guerra, D.D., Yu, S., Wogulis, M., Kraft, E., Frommer, W.B., et al. (2012) The ubiquitin E3 ligase LOSS OF GDU2 is required for GLUTAMINE DUMPER1-induced amino acid secretion in Arabidopsis. *Plant Physiol.* 158: 1628–1642.
- Sakamoto, T., Kamiya, T., Sako, K., Yamaguchi, J., Yamagami, M. and Fujiwara, T. (2011) Arabidopsis thaliana 26S proteasome subunits RPT2a and RPT5a are crucial for zinc deficiency-tolerance. *Biosci. Biotechnol. Biochem.* 75: 561–567.
- Sako, K., Maki, Y., Kanai, T., Kato, E., Maekawa, S., Yasuda, S., et al. (2012) Arabidopsis RPT2a, 19S proteasome subunit, regulates gene silencing via DNA methylation. *PLoS One* 7: e37086.
- Santner, A. and Estelle, M. (2010) The ubiquitin-proteasome system regulates plant hormone signaling. *Plant J.* 61: 1029–1040.
- Sato, T., Maekawa, S., Yasuda, S., Domeki, Y., Sueyoshi, K., Fujiwara, M., et al. (2011) Identification of 14-3-3 proteins as a target of ATL31 ubiquitin

- ligase, a regulator of the C/N response in Arabidopsis. *Plant J.* 68: 137–146.
- Sato, T., Maekawa, S., Yasuda, S., Sonoda, Y., Katoh, E., Ichikawa, T., et al. (2009) CNI1/ATL31, a RING-type ubiquitin ligase that functions in the carbon/nitrogen response for growth phase transition in Arabidopsis seedlings. *Plant J.* 60: 852–864.
- Schat, H., Vooijs, R. and Kuiper, E. (1996) Identical major gene loci for heavy metal tolerances that have independently evolved in different local populations and subspecies of *Silene vulgaris*. *Evolution* 50: 1888–1895.
- Sharma, B., Joshi, D., Yadav, P.K., Gupta, A.K. and Bhatt, T.K. (2016) Role of ubiquitin-mediated degradation system in plant biology. *Front. Plant Sci.* 7: 806.
- Shin, L.J., Lo, J.C., Chen, G.H., Callis, J., Fu, H.Y. and Yeh, K.C. (2013) IRT1 DEGRADATION FACTOR1, a RING E3 ubiquitin ligase, regulates the degradation of IRON-REGULATED TRANSPORTER1 in Arabidopsis. *Plant Cell* 25: 3039–3051.
- Sirko, A., Wawrzyńska, A., Rodríguez, M.C. and Sętkas, P. (2014) The family of LSU-like proteins. *Front. Plant Sci.* 5: 774.
- Smalle, J., Kurepa, J., Yang, P., Emborg, T.J., Babiychuk, E., Kushnir, S., et al. (2003) The pleiotropic role of the 26S proteasome subunit RPN10 in Arabidopsis growth and development supports a substrate-specific function in abscisic acid signaling. *Plant Cell* 15: 965–980.
- Smalle, J. and Vierstra, R.D. (2004) The ubiquitin 26S proteasome proteolytic pathway. *Annu. Rev. Plant Biol.* 55: 555–590.
- Solano, R., Stepanova, A., Chao, Q. and Ecker, J.R. (1998) Nuclear events in ethylene signaling: a transcriptional cascade mediated by ETHYLENE-INSENSITIVE3 and ETHYLENE-RESPONSE-FACTOR1. *Genes Dev.* 12: 3703–3714.
- Stone, S.L. (2014) The role of ubiquitin and the 26S proteasome in plant abiotic stress signaling. *Front. Plant Sci.* 5: 135.
- Stracke, R., Werber, M. and Weisshaar, B. (2001) The R2R3-MYB gene family in *Arabidopsis thaliana*. *Curr. Opin. Plant Biol.* 4: 447–456.
- Sun, C.W. and Callis, J. (1997) Independent modulation of *Arabidopsis thaliana* polyubiquitin mRNAs in different organs and in response to environmental changes. *Plant J.* 11: 1017–1027.
- Swiatowy, W. and Jagodzinski, P.P. (2018) Molecules derived from tRNA and snoRNA: Entering the degradome pool. *Biomed. Pharmacother.* 108: 36–42.
- Takahashi, H., Kopriva, S., Giordano, M., Saito, K. and Hell, R. (2011) Sulfur assimilation in photosynthetic organisms: molecular functions and regulations of transporters and assimilatory enzymes. *Annu. Rev. Plant Biol.* 62: 157–184.
- Thrower, J.S., Hoffman, L., Rechsteiner, M. and Pickart, C.M. (2000) Recognition of the polyubiquitin proteolytic signal. *EMBO J.* 19: 94–102.
- Tian, T., Liu, Y., Yan, H., You, Q., Yi, X., Du, Z., et al. (2017) agriGO v2.0: a GO analysis toolkit for the agricultural community, 2017 update. *Nucleic Acids Res.* 45: W122–W129.
- Torres, A.G., Reina, O., Stephan-Otto Attolini, C. and Ribas de Pouplana, L. (2019) Differential expression of human tRNA genes drives the abundance of tRNA-derived fragments. *Proc. Natl. Acad. Sci. USA* 116: 8451–8456.
- Ueda, M., Matsui, K., Ishiguro, S., Sano, R., Wada, T., Paponov, I., et al. (2004) The HALTED ROOT gene encoding the 26S proteasome subunit RPT2a is essential for the maintenance of Arabidopsis meristems. *Development* 131: 2101–2111.
- Üstün, S., Sheikh, A., Gimenez-Ibanez, S., Jones, A., Ntoukakis, V. and Börnke, F. (2016) The proteasome acts as a hub for plant immunity and is targeted by pseudomonas type III effectors. *Plant Physiol.* 172: 1941–1958.
- Vaahtera, L. and Brosche, M. (2011) More than the sum of its parts—how to achieve a specific transcriptional response to abiotic stress. *Plant Sci.* 180: 421–430.
- Vierstra, R.D. (2009) The ubiquitin-26S proteasome system at the nexus of plant biology. *Nat. Rev. Mol. Cell Biol.* 10: 385–397.
- Walley, J.W. and Dehesh, K. (2010) Molecular mechanisms regulating rapid stress signaling networks in Arabidopsis. *J. Integr. Plant Biol.* 52: 354–359.
- Wang, Y., Li, H.X., Sun, Q.X. and Yao, Y.Y. (2016) Characterization of small RNAs derived from tRNAs, rRNAs and snoRNAs and their response to heat stress in wheat seedlings. *PLoS One* 11: e0150933.
- Watanabe, M. and Hoefgen, R. (2019) Sulphur systems biology-making sense of omics data. *J. Exp. Bot.* 70: 4155–4170.
- Wawrzyńska, A., Lewandowska, M., Hawkesford, M.J. and Sirko, A. (2005) Using a suppression subtractive library-based approach to identify tobacco genes regulated in response to short-term sulphur deficit. *J. Exp. Bot.* 56: 1575–1590.
- Wawrzyńska, A. and Sirko, A. (2014) To control and to be controlled: understanding the Arabidopsis SLIM1 function in sulfur deficiency through comprehensive investigation of the EIL protein family. *Front. Plant Sci.* 5: 575.
- Wawrzyńska, A. and Sirko, A. (2016) EIN3 interferes with the sulfur deficiency signaling in *Arabidopsis thaliana* through direct interaction with the SLIM1 transcription factor. *Plant Sci.* 253: 50–57.
- Wojcik, C. and DeMartino, G.N. (2003) Intracellular localization of proteasomes. *Int. J. Biochem. Cell Biol.* 35: 579–589.
- Xu, F.Q. and Xue, H.W. (2019) The ubiquitin-proteasome system in plant responses to environments. *Plant Cell Environ.* 42: 2931–2944.
- Yoo, S.D., Cho, Y.H., Tena, G., Xiong, Y. and Sheen, J. (2008) Dual control of nuclear EIN3 by bifurcate MAPK cascades in C2H4 signalling. *Nature* 451: 789–795.
- Zientara, K., Wawrzyńska, A., Łukomska, J., López-Moya, J.R., Liszewska, F., Assunção, A.G.L., et al. (2009) Activity of the AtMRP3 promoter in transgenic *Arabidopsis thaliana* and *Nicotiana tabacum* plants is increased by cadmium, nickel, arsenic, cobalt and lead but not by zinc and iron. *J. Biotechnol.* 139: 258–263.